

Reinforcement of model filled elastomers: synthesis and characterization of the dispersion state by SANS measurements

J. Berriot^a, H. Montes^{a,*}, F. Martin^a, M. Mauger^a, W. Pyckhout-Hintzen^b,
G. Meier^b, H. Frielinghaus^b

^aESPCI, Lab de Physico-Chimie Structurale et Macromoléculaire, PCSM UMR 7615, 10 Rue Vauquelin, Paris Cedex 05 75005, France

^bIFF, Forschungszentrum Juelich, D-52428 Jülich, Germany

Received 12 December 2002; received in revised form 10 April 2003; accepted 30 May 2003

Abstract

This work is the first part of a study devoted to the understanding and the determination of the molecular mechanisms that are at the origin of the specific properties shown by reinforced elastomers. Different model filled elastomers composed of cross-linked polyethylacrylate chains reinforced with grafted silica nanoparticles were prepared varying the reactivity of the coupling agent with the ethylacrylate monomers. They were synthesized applying and adapting the method developed by Ford et al. [11] which consists to polymerize a colloidal suspension of grafted silica particles in acrylate monomers. In this paper we will present how filled elastomers having different dispersion states can be prepared whilst keeping the same interactions between the particles and the polymer chains. The dispersion states were characterized by Small Angle Neutron Scattering. We found that there are two opposite effects which control the final dispersion state of these filled elastomers during the polymerization. The first one is a depletion mechanism favoring the formation of aggregates. The second one is a repulsive steric interaction due to the growth of polymer chains from the particle surfaces avoiding contacts between the silica inclusions. Using these results we can prepare sets of samples having the same particle/matrix interface but different dispersions states. By comparing their mechanical properties we should be able to estimate the relative weight of the dispersion state quality and the one of the particle/matrix interface on the mechanical behavior of these filled elastomers.

© 2003 Elsevier Science Ltd. All rights reserved.

Keywords: Filled elastomers; Dispersion state; Small angle neutron scattering

1. Introduction

The addition of solid inclusions deeply modifies the mechanical properties of an elastomer matrix. Reinforced elastomers exhibit specific mechanical properties compared to those shown by an elastomer matrix. For instance their modulus sensitively decreases at very small deformations (deformations lower than 1%), while the one of the non-reinforced matrices remains constant. This well known feature is called the Payne effect. The second specific behavior is the Mullins effect which is associated with the hysteresis appearing between the first (virgin) and the second stress-strain curves. A lot of work were devoted to the understanding of these two specific behaviors. These previous studies have shown that the mechanical properties

are strongly controlled by the two following parameters. The first one is the nature of the interactions between the polymer chains and the particle surface [1–5]. These interactions are controlled by the chemistry of the particle surface. If grafted particles are used to reinforce the polymer matrix, the interactions depend thus on the nature of the coupling agent covering the particles surface. The second parameter, which influences the mechanical properties of the filled elastomers is the quality of the dispersion state of the particles in the elastomer matrix [1,6–10]. The reference [1] gives a very good overview of all the main results measured on many filled elastomers.

However, most of these studies were performed on commercial filled samples prepared by mixing together the polymer chains and the particles. Indeed, the change of the chemistry at the particle surface often leads to a change of the dispersion state. This procedure does not allow to

* Corresponding author. Tel.: +33-1-4079-4687; fax: +33-1-4079-4686.
E-mail address: helene.montes@espci.fr (H. Montes).

analyze separately the influence of the two parameters—particle/matrix interactions and dispersion state quality.

We prepared thus model filled-elastomers for which it was possible to vary separately the chemistry at the particle surface and the dispersion state in order to determine the relative weight of these two parameters on the mechanical behavior. Such samples were prepared by using and adapting the procedure developed by Ford [11]. This method consists to polymerize a concentrated dispersion of grafted silica particles in acrylate monomers. Such an approach was already used by Pu et al. [12] to investigate the effect of organized and disordered dispersion states on the stress–strain curves of filled systems. We prepared different samples, varying the nature of the coupling agent grafted onto the particle surfaces. Since the dispersion state strongly influences the mechanical properties it is necessary to carefully characterize it. In this aim we performed Small Angle Neutron Scattering measurements (SANS). In this paper we present how we prepared, keeping the interactions between the particles and the polymer chains at constant, model-filled elastomers with different dispersion states.

The paper is organized as follows. In the first part, we describe the procedures used to prepare several kinds of filled elastomers having different dispersion states. The second part presents the characterization of the dispersion state made by Small Angle Neutron Scattering. The different parameters controlling the dispersion state are analyzed in Section 4.

2. Experimental section

2.1. Sample preparation

The different pathways used for the sample preparation are presented in Fig. 1. More details are given below.

2.1.1. Main steps of the filled elastomer synthesis

Spherical, weakly polydisperse particles of colloidal silica were prepared following the procedure developed by Stöber [13]. Part of them were kindly provided by Rhodia (Aubervilliers, France). Silica particles with varying diameter were prepared and characterized by Small Angle Neutron Scattering. Their mean diameters range from 45 to 80 nm.

Filled elastomers were prepared from these colloidal silica solutions following and adapting the general procedure developed by Ford et al. [11].

First, short silane molecules are grafted onto the silica particle surface using a dilute silica dispersion having a particle volume fraction of 2%. Three kinds of non-polar coupling agents were used: the 3-methacryloxy-propyl-trimethoxysilane (TPM), the 3 methacryloxy propyl dimethylchlorosilane (MCS) and the acetoxethyl dimethylchlorosilane (ACS). The solvent in which the grafting reaction is performed depends on the coupling

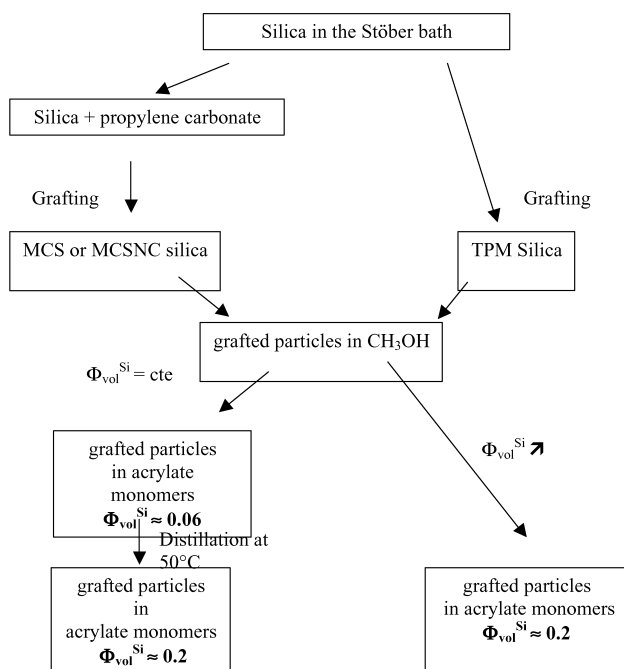


Fig. 1. Schematic presentation of the main steps which were followed for the preparation of a concentrated parent solution of grafted silica particles in acrylate monomers.

agent. For the TPM molecules the grafting step is carried out in the initial Stöber solution which is a mixture of water, ammoniac and ethanol. The grafting reaction of the two coupling agents MCS and ACS requires to work in an aprotic solution. In this aim, the colloidal silica is transferred by dialysis in propylene carbonate prior to the grafting reaction. Quantification of the amount of grafted coupling agent was determined by elemental analysis comparing the carbon and silicon contents of the non-grafted and grafted silica particles. The results are given in Table 1.

The dispersion of grafted silica particles is first transferred to methanol and then to the ethylacrylate monomer by successive dialysis. Finally, a photoinitiator (Irgacure (Ciba, France)) (0.1 wt% to monomer) and a cross-linker—the diacrylate butanediol—are added to this dispersion in order to achieve the polymerization and the reticulation respectively under UV illumination. Irrespective of the silica volume fraction, the concentration of crosslinker was kept equal to 0.3% per mol of acrylate monomer. The grafted silica dispersion in acrylate is syringed into a cell formed by two glass moulds. The cell is placed on a rotating plate and is irradiated during 4 h by a fixed medium pressure 450 W Hg lamp. The polymerization and the reticulation of the polyacrylate chains occur simultaneously.

2.1.2. Preparation of varying concentrated silica dispersions

From each initial solution of grafted silica particles, we prepared a concentrated dispersion of silica in acrylate

Table 1
Characteristics of the reinforced sample sets

Serie name	Silica reference	Graft type	Graft density (nm ⁻²)	Concentration procedure
ACS/C	Si_III	ACS	2	(C)
MCS_I/C	Si_I	MCS	1.6 ± 0.5	(C)
MCS_II/H	Si_II	MCS	2.8 ± 0.5	(H)
MCS_III/C	Si_III	MCS	<1	(C)
TPM_I/H	Si_II	TPM	3.3 ± 0.5	(H)
TPM_II/H	Si_III	TPM	7.8 ± 0.8	(H)
TPM_III/C	Si_IV	TPM	10.5 ± 3	(C)

(H) corresponds to a distillation in acrylate monomer at 50 °C; (C) signifies a concentration step during the transfer from methanol to acrylate monomers by dialysis.

monomer (around 0.2 in volume). This parent solution was then diluted with acrylate monomer in order to obtain several solutions with varying silica concentrations which are then polymerized.

The transfer of the grafted silica particles from the methanol to the acrylate monomers is accompanied by a natural increase of the silica concentration in the colloidal solution. The silica volume fraction variations can be controlled by directly adding acrylate monomers in the dialysis tube. The colloidal suspension obtained at the end of the dialysis are thus more or less diluted depending on the acrylate monomers volume added during this step.

We drew two different ways to obtain a concentrated parent silica/acrylate solution.

The first procedure consists in concentrating the solution during dialysis in the acrylate monomers such that a solution of 0.2 silica volume fraction is obtained. Such samples will be noted 'C'.

The second way consists in maintaining the solution diluted during the dialysis in the acrylate monomers and in concentrating the silica dispersion afterwards by distillation. By this way the silica volume fraction after the dialysis in acrylate monomers is around 0.06 in volume. This solution is concentrated by distillation carried out at a temperature of 50 °C. The distillation is stopped when a dispersion containing 0.2 silica volume fraction is obtained. No polymerization of the monomers is observed at a macroscopic scale during this step. The corresponding samples will be designed by 'H'.

2.1.3. Chemical structure of the particle/polymer interface

2.1.3.1. Chemical structure of the covering. The chemical structure of the coupling agent at the silica surface was analyzed by ²⁹Si NMR. The ²⁹Si NMR measurements were performed using the following pulse sequence ($\pi/2$, τ , acquisition) and applying a broad band decoupling on the protons.

The chemical shift δ of one ²⁹Si atom depends both on the number of oxygen atom directly linked to it and on the number of silicon atoms connected via 2 covalent bonds. By ²⁹Si NMR experiment we detect three kinds of silicon atoms for silica particles designated by Q²(= (RO)₂Si(OSi)₂),

Q³(= (RO)₁Si(OSi)₃) and Q⁴(= Si(OSi)₄). Their chemical shift are around $\delta = -90, -100, -110$ ppm, respectively.

The TPM coupling agent has three methoxy groups which become three reacting hydroxyl groups after hydrolysis in the initial solution (H₂O, ethanol, NH₄OH). One TPM molecule can then react with three hydroxyl groups belonging to neighboring TPM molecules or located at the silica surface. According to whether the silicon atom of the TPM is connected to one (T¹), two (T²) or three (T³) OSi groups, its chemical shifts is different: $\delta = -48$ ppm (T¹), $\delta = -57$ ppm (T²) and $\delta = -65$ ppm (T³). The ²⁹Si NMR spectra of TPM grafted silica showed the presence of silicon atoms of the type (T²) and (T³) for the TPM molecules. The silicon of type T³ represents 70% of the TPM silicon. There is thus around the particle a dense shell composed of polycondensated TPM molecules. It results that for the TPM coupling agent the amount of grafted molecules can be larger than the number of hydroxyl groups at the silica surface. These results agree with previous observations made by Ford [14]

At the opposite, the MCS and ACS coupling agents have only one group that can react with the hydroxyl groups. In this case there is no polycondensation between neighboring molecules. The coupling agents form brushes along the particle surface. The ²⁹Si spectra of MCS grafted silica show the only presence of silicon atoms of type M which correspond to (SiO)–Si–(CH₃)₂R groups and which appear at a chemical shift $\delta = 24$ ppm.

2.1.3.2. Interaction of the grafters with the polyacrylate chains. TPM and MCS molecules contain one methacrylate group which can react with the acrylate monomers during the polymerisation step. On the contrary, the ACS coupling agent does not possess a methacrylate end. NMR and swelling measurements showed that the TPM or MCS silica particles are covalently bonded to the acrylate matrix [15–17] while the ACS silica particles are not connected to the elastomer network.

We prepared several sets of filled elastomers differing by their particle diameters, the chemical nature of the grafted and the concentration procedure. A set of samples corresponds to reinforced elastomers prepared from the same initial grafted silica solution applying a given

concentration procedure. One set of filled materials is composed by samples having silica volume fraction between 0.06 and 0.2.

In this work we will study in which way the final dispersion state of the particles in the acrylate matrix depends on the chemical nature of the grafter and on the concentration procedure applied.

2.2. Sans measurements

The SANS measurements were performed on the KWS1 and KWS2 spectrometers at the Forschungszentrum Juelich GmbH). The scattered intensity was detected at room temperature for values of the wavevector q between 2×10^{-3} and $2 \times 10^{-1} \text{ \AA}^{-1}$. The measured intensities were calibrated to an absolute standard in order to get absolute units.

The form factors of the silica particles were measured on very diluted solutions containing 0.7% in volume of silica particles in desionised water. The characteristic of the particles were determined by fitting the experimental data with the theoretical form factors of spherical objects taking the polydispersity into account. Moreover, the theoretical spectra were convoluted with the corresponding resolution function which includes the wavelength spread of 15% and the geometrical factors influencing the resolution. Whatever the set of reinforced systems, the measurements of the scattered intensity of the filled samples and of the form factor of the corresponding silica particles were performed on the same spectrometer.

The respective scattering length b_A of the silica particles and of the acrylate monomers were determined using the following relation: $b_A = \sum_i b_i/v_A$ where b_i are the scattering length of the several atoms forming one molecule of component A and v_A is its molecular volume. We deduce then that $b_{Si} = 3.1 \times 10^{+10} \text{ cm}^{-2}$ and $b_{EA} = 1.00 \times 10^{+10} \text{ cm}^{-2}$ where b_{Si} , b_{EA} are the scattering lengths for silica and ethylacrylate monomers respectively.

3. SANS measurements

In a neutron scattering experiment, the scattered intensity from a sample is directly related to the scattering length of the components forming the system, their concentration and their relative positions in the sample. Let's consider a two components system, such that the volume fraction of the component A is ϕ_A and the volume fraction of the component B is $(1 - \phi_A)$. The scattered intensity is then proportional to the cross section:

$$\frac{d\sigma(q)}{d\Omega} = b^2 \sum_{\alpha,\beta} \sum_{i,j}^{n,n} \langle \exp[iq(\mathbf{r}_i^\alpha - \mathbf{r}_j^\beta)] \rangle \quad (1)$$

$$\text{with } b = (b_A - b_B(v_A/v_b)) \quad (2)$$

where b_A and b_B are the scattering lengths of the

components A and B, and \mathbf{r}_i^α the position of the i th monomer of species α . v_A and v_B are the monomer volume of the component A and B respectively. In our systems the contrast originates from the difference between the scattering lengths between the polymer and the silica particles. Therefore, the SANS measurements give the Fourier transform of the silica density.

3.1. Theoretical section

For a suspension of spherical particles the differential cross section can be written:

$$\frac{d\sigma(q)}{d\Omega} = b^2 \phi V_{Si} P(q) S(q) \quad (3)$$

where $P(q)$ is the form factor of the silica particles, ϕ the volume fraction of silica particles, V_{Si} the volume of one silica particle and $S(q)$ the structure factor of the silica particles. $S(q)$ is the Fourier transform of the correlation function of the mass center of the silica particles.

For very dilute solutions, as there is no interaction between silica particles, $S(q) = 1$ and the scattered intensity is then only dependent on the form factor $P(q)$. We assume that upon measuring $P(q)$ in dilute and well-dispersed sample, we can deduce for more concentrated solutions the structure factor $S(q)$ of the silica particles which is directly related to the dispersion state of the particles.

For concentrated suspensions of spherical particles having a diameter D , the structure factors contribute to the scattered intensity for $q < 2\pi/D$.

If the particles have a liquid-like order, the structure factor has a correlation peak at q_{\max} which characterizes the average distance between particles.

As the particles are badly dispersed in the polymer matrix and form aggregates, the structure factor $S(q)$ can be written as the product of the intra-aggregate structure factor $S_{\text{intra}}(q)$ with the inter-aggregate structure factor $S_{\text{agg}}(q)$: $S(q) = S_{\text{intra}}(q) \times S_{\text{agg}}(q)$ [18]. The intra contribution $S_{\text{intra}}(q)$ corresponds to the form factor of the aggregates composed of many spherical particles. $S_{\text{intra}}(q)$ differs thus from the form factor $P(q)$ of one spherical particle. If the aggregates have a liquid-like order the inter-aggregate structure factor $S_{\text{agg}}(q)$ has also a correlation peak whose position q_{\max} is related to the size of the aggregates according the relation: $N_{\text{agg}} \approx (2\pi/q_{\max})^3 \phi/V_{Si}$ where N_{agg} is the mean number of aggregation, ϕ the volume fraction of particles, V_{Si} the volume of one particle.

3.2. Experimental results

In the following we will call the differential cross section as $I(q)$.

3.2.1. Silica form factor

The form factors of the silica particles were measured on very dilute solutions containing a volume fraction of

non-grafted silica particles of 0.007 in desionised water. In this case, there is no interaction between the particles and $S(q) = 1$. The total scattering cross section is then proportional to the form factor $P(q)$ of the silica particles.

Fig. 2 (Table 2) shows the scattering intensities of the three kinds of silica particles among the four batches we used to reinforce the poly(ethylacrylate) matrices. The intensities were shifted by an arbitrary coefficient for a better visibility of all the curves.

The mean diameter and the size polydispersity of the particles were determined by fitting the experimental data with the form factor of spherical objects. The size polydispersity was described using a Schultz distribution function given by:

$$f(D) = \left[\frac{t+1}{D_{\text{mean}}} \right] \frac{D^t}{t!} \exp\left(-\left[\frac{t+1}{D_{\text{mean}}} \right] D\right) \quad (4)$$

where D_{mean} is the mean number diameter of the particles, t is the Schulz width factor. Moreover the fits include the resolution function of the spectrometers.

The solid lines correspond to the best fitting obtained by adjusting the two parameters D_{mean} and t of the Schulz distribution function. Their values are given in Table 2 and the corresponding distribution functions are plotted in the inset of Fig. 2. We have also determined the parameter σ which corresponds to the ratio D/D_{mean}

Table 2

Mean size and polydispersity of the different silica particles measured by SANS

Silica name	D_{mean} (nm)	t	σ
Si_I	45	60	0.12
Si_II	50	70	0.12
Si_III	54	70	0.11
Si_IV	80	55	0.13

such that $f(D)/f(D_{\text{mean}})$ is equal to 0.5. σ characterizes the size polydispersity.

At high q values, the intensity varies as q^{-4} according to the Porod law. We have found no difference between the intensity scattered by grafted and non-grafted silica particles. The silica particles are only weakly polydisperse.

3.2.2. Structure factors of the reinforced elastomers

For all the filled elastomers, the SANS measurements showed that at high q values the intensity follows a q^{-4} power law. Knowing the form factor of the silica particles, we can then determine using Eq. (4) the structure factor for each filled sample. The structure factor $S(q)$ is deduced by dividing the measured intensity by the form factor of the silica particle determined experimentally.

We will analyse the effect of the synthesis procedure, the

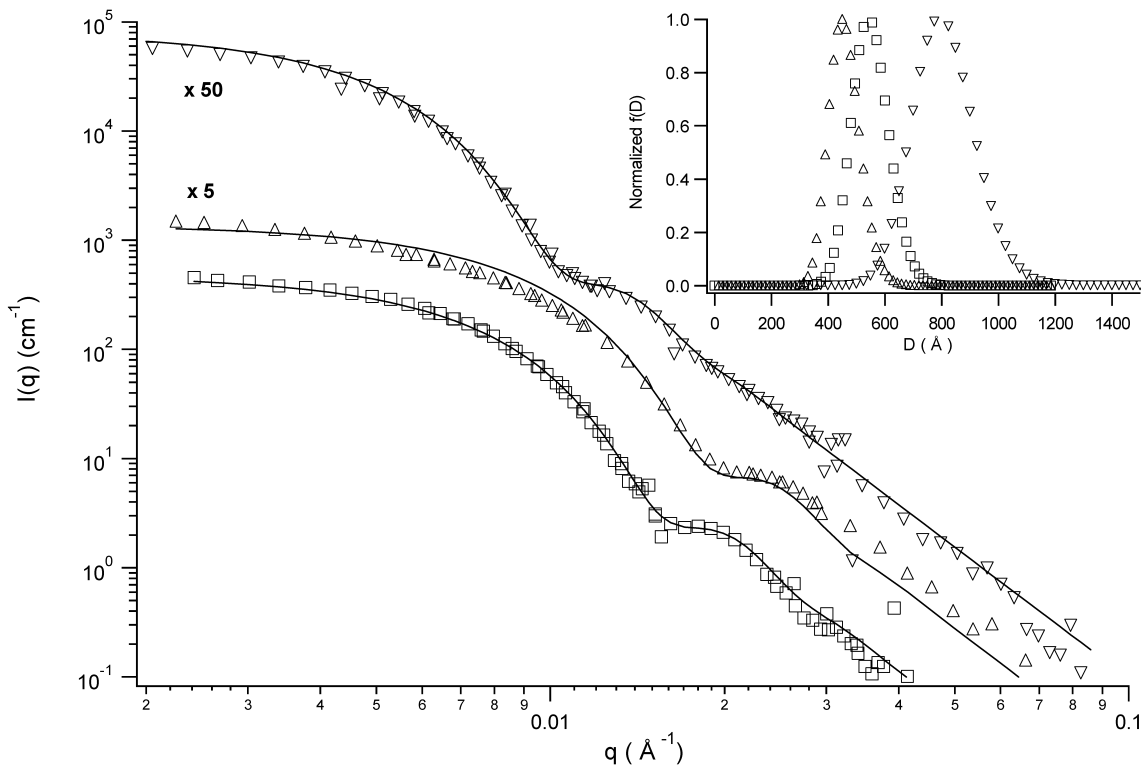


Fig. 2. Form factor of the different Stöber silica particles: (Δ): Si_I; (\square) Si_III; (∇): Si_IV. The solid lines correspond to the theoretical form factor of spherical particles including the resolution function of the spectrometer. The polydispersity was taken into account with a Schultz size-distribution function. The corresponding mean diameters D_{mean} are listed in Table 2 for each kind of particles as well as the parameters of polydispersity t and D_{σ} . The corresponding Schultz distribution functions are presented in the inset.

influence of the coverage ratio and of the chemical nature of the grafters on the final dispersion state.

3.2.2.1. Influence of the synthesis procedure on the dispersion state. We have distinguished two synthesis procedures corresponding to two different concentration steps. The first samples referred to as ‘C’ were obtained from a parent solution that was concentrated during the dialysis in the acrylate monomers. The second kind of systems referred to as ‘H’ were prepared from a concentrated silica/acrylate dispersion obtained after distillation at 50 °C of a dilute silica/acrylate solution.

We will compare in this section the dispersion state of samples reinforced with silica particles whose surface is totally covered by grafted molecules. In this case, the samples are transparent whatever the concentration procedure.

In order to correct for differences due to different silica volume fractions ϕ and particle diameters we will plot the scattered intensity normalized by the silica volume fraction ϕ and the volume of one silica particle $V_{\text{si}}(I(q)/\phi V_{\text{si}})$ versus the reduced variable qD_{mean} .

In Fig. 3 we compared the intensity scattered by two samples of the set MCS_I/C reinforced with 0.07 (vol) (filled circles) and 0.24 (vol) (open circles) of silica particles to the one measured on one MCS_II/H sample containing a silica volume fraction of 0.10. In the inset the experimental data measured on two MCS_II/H samples ($\phi = 0.18$ and

0.10) are compared to the normalized form factor of the corresponding silica particles.

We will now pick out the main features of these curves

- for $qD_{\text{mean}} > 2\pi$, as the form factor is predominant ($S(q) = 1$), the curves are similar.
- for $qD_{\text{mean}} < 2\pi$ as the structure factor contributes to the scattered intensity the intensity scattered by the MCS_II/H samples is sensibly larger than the one measured with the MCS_I/C samples.
- A structure peak is observed for the MCS_I/C samples. Its position q_{max} decreases as the silica concentration decreases. No structure peak is observed for the MCS_II/H samples whatever the silica concentration.
- At low q values, the values of the experimental curves remain lower than the values of the normalized form factor.

Equivalent observations are made with C and H samples reinforced with TPM coated silica particles. Fig. 4 shows the data measured on one TPM_III/C samples and one TPM_II/H material having the same silica volume fraction ($\phi = 0.10$). These results show that the particle dispersion state of the H sample is worse than the one observed in the C samples.

We will now analyze more in detail the quality of the different dispersion states. For this purpose we will consider the quantity $(I(q, \phi)/\phi b^2)/(I(q, \phi_1)/\phi_1 b_1^2)$ where $I(q, \phi)$ is

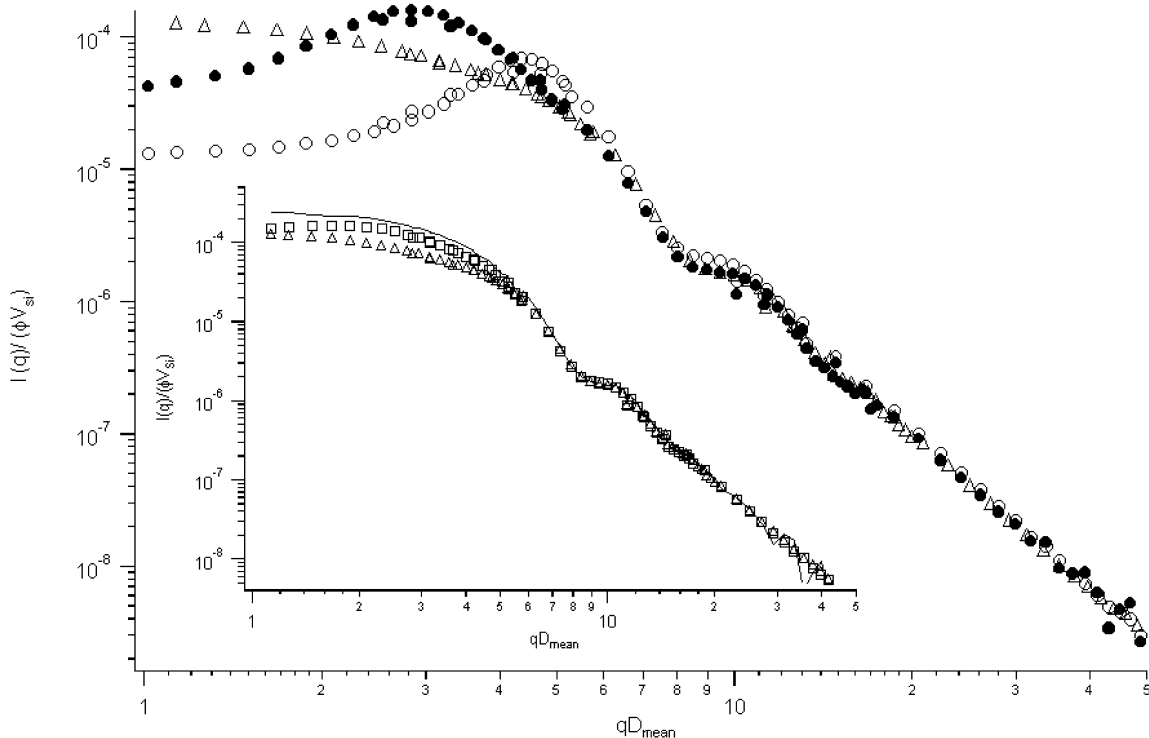


Fig. 3. Variation of the normalized and reduced scattering intensity $I(qD_{\text{mean}})/\phi V_{\text{si}}$ with the variable qD_{mean} for MCS_I/C and MCS_II/H. MCS_I/C: (○) $\phi = 0.24$, (●) $\phi = 0.07$. MCS_II/H samples: (△): $\phi = 0.10$. Inset: Comparison of the normalized scattering intensities of the MCS_II/H samples with the form factor of the Si_II silica particles deduced from measurements performed on very dilute solutions (see Section 3.2.2.1). MCS_II/H samples: (△): $\phi = 0.10$. (□): $\phi = 0.18$. The normalized form factor of the Si_II particles is plotted as a continuous line.

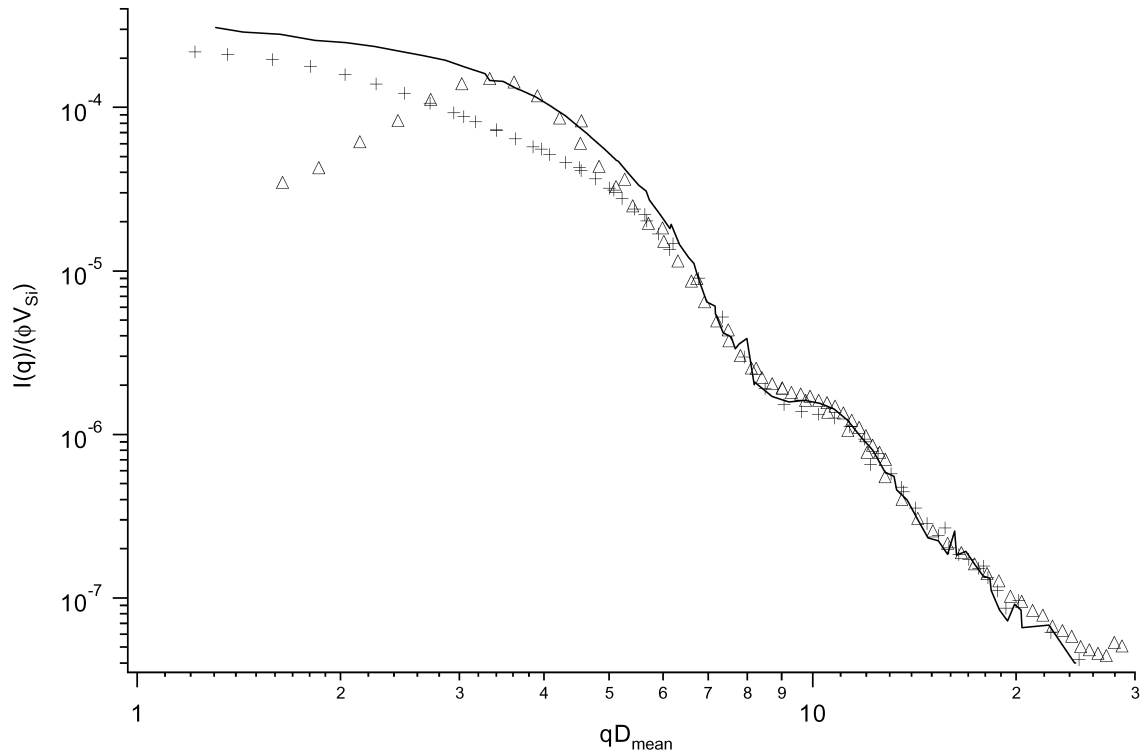


Fig. 4. Normalized scattering intensities $I(qD_{\text{mean}})/\phi V_{\text{Si}}$ versus qD_{mean} as before for one TPM_III/C (Δ) sample and one TPM_II/H sample (+) having the same volume fraction $\phi = 0.10$. The normalized form factor of the Si_III deduced from the measurements on dilute solution (see Section 3.2.1) is plotted as a continuous line.

the scattered intensity measured on reinforced elastomers having a silica concentration ϕ and a scattering contrast b . $I(q, \phi_1)$ corresponds to the form factors measured on the dilute silica solutions of silica concentration ϕ_1 and scattering contrast b_1 . This quantity corresponds in a first approximation to the structure factor of the reinforced elastomer. We will call $(I(q, \phi)/\phi b^2)/(I(q, \phi_1)/\phi_1 b_1^2)$ as $S(q)$ in the following.

The structure factors obtained on the TPM_III/C samples for the two concentrations $\phi = 0.18$ and $\phi = 0.10$ are presented in Fig. 5a. In addition to a large structure peak visible at q_{max} , ($q_{\text{max}}D_{\text{mean}} = 4.5$ for $\phi = 0.18$ and $q_{\text{max}}D_{\text{mean}} = 3.6$ for $\phi = 0.10$), we observed, that the second structure peak ($qD_{\text{mean}} = 9$) varies with the silica concentration. We deduce that the particles have in the C samples a structure similar to the one of a repulsive sphere suspension but with an exclusion diameter D_{exc} larger than their own diameter. The average value of the exclusion diameter can be deduced from the position of the structure peak q_{max} according to the relation $D_{\text{exc}} = 2\pi/q_{\text{max}}$. In Table 3 the position of the structure peak and the corresponding values of D_{exc} measured for each sample set at different particle concentrations are listed, together with a comparison of the experimental values of D_{exc} to the average distance between the centers of two particles L calculated using the relation $L = D_{\text{mean}}(\phi_{\text{cp}}/\phi)^{1/3}$ where ϕ_{cp} is the concentration at the close packing. (The values of the ratio L/D_{mean} are given in Table 3). We have chosen for ϕ_{cp}

its value for a cubic arrangement ($\phi_{\text{cp}} = 0.52$) and observed that the ratio $D_{\text{exc}}/D_{\text{mean}}$ is close to the theoretical values L/D_{mean} for the MCS_I/C and TPM_III/C samples.

In the H systems, the dispersion state is worse than the ones observed on the C samples. However, we do not observe a strong increase of the scattered intensity at low q values. Fig. 5b shows the structure factors $S(q)$ for two TPM_II/H samples having a silica volume fraction of 0.13 and 0.18. For qD_{mean} values larger than 6 the structure factors measured at the two concentrations are the same. In this q range, we observe a peak at $qD_{\text{mean}} = 7$. Its amplitude and its position do not change with the silica concentration. At $q_1D_{\text{mean}} \approx \pi$ the structure factors show a shallow minimum ($S(q_1) \approx 0.4$ for $\phi = 0.18$ and $S(q_1) \approx 0.5$ for $\phi = 0.10$). Furthermore at $q < \pi/D_{\text{mean}}$ the structure factors increase slowly for decreasing qD_{mean} values following a power law $(qD_{\text{mean}})^{-0.7}$. We do not observe in this q range a

Table 3

Variation of the structure peak position Q_{max} and the exclusion diameter D_{exc} with silica concentration for well dispersed samples

Set name	Silica concentration (volume)	Q_{max} (\AA^{-1})	D_{exc} (\AA)	$D_{\text{exc}}/D_{\text{mean}}$	L/D_{mean}
TPM_III/C	0.09	0.0046	1400	1.75	1.8
	0.18	0.006	1100	1.375	1.42
MCS_I/C	0.07	0.007	850	1.9	1.95
	0.24	0.011	540	1.2	1.3

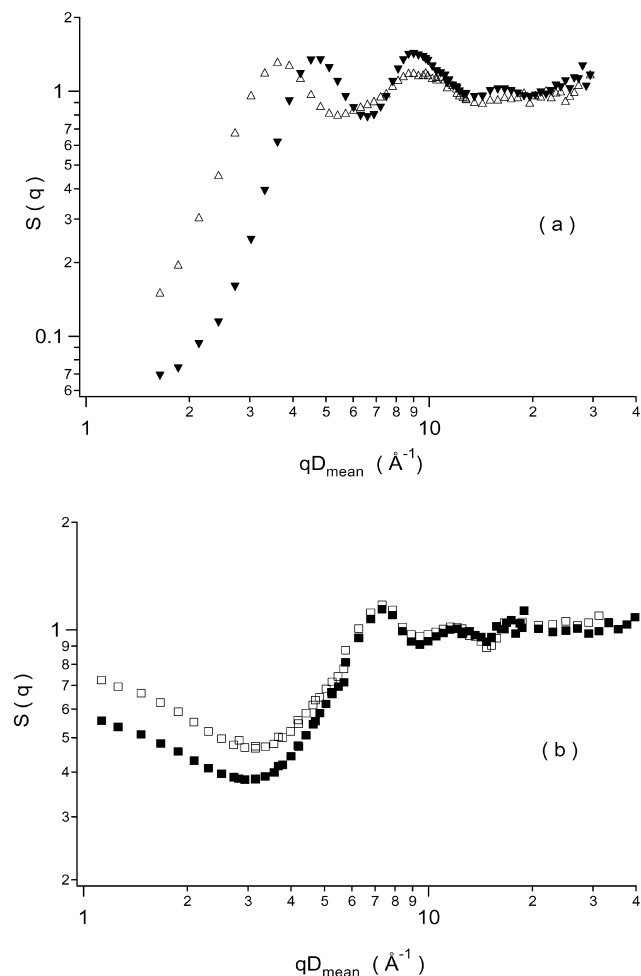


Fig. 5. (a) The structure factors deduced for two TPM_III/C samples are shown in the inset: (Δ): $\phi = 0.10$ and (\blacktriangledown): $\phi = 0.18$. (b) Variation of the structure factors versus qD_{mean} for two samples of the set TPM_II/H containing: (\square): $\phi = 0.13$ and (\blacksquare): $\phi = 0.18$.

structure peak as for the C samples. This feature can be understood as being the sign of the presence of small aggregates. The low value of the exponent (-0.7) indicates that few aggregates having a linear shape (doublet, triplets) would coexist with single particles. Similar observations were made for the TPM_I/H and MCS_II/H samples. These results agree with recent simulations performed by Oberdisse et al. [19] comparing the intra-aggregate structure factors of aggregates with varying compacity and shape. These authors show that the structure factor of fractal aggregates shows a broader order peak at $q \approx 2\pi/D_{\text{mean}}$ and increases slowly at low q after a shallow minimum.

The concentration step influences thus the final dispersion state of our filled elastomers. A natural concentration occurring during the dialysis in the acrylate monomers leads to samples having a very good dispersion state while a concentration step using a distillation at 50°C favors the formation of linear aggregates in the filled sample.

3.2.2.2. Influence of the coverage ratio of the silica surface.

In this section we analyze the influence of the coverage ratio on the dispersion state quality. In this aim we compared samples of the set MCS_I/C and MCS_III/C. They are obtained using the same concentration procedure and they are reinforced with silica particles grafted with the same grafted molecules. For the MCS_I/C samples, the surface of the silica particles is totally covered by grafted molecules while the coverage is only partial for the MCS_III/C samples.

Fig. 6 shows the normalized scattered intensities $I(qD_{\text{mean}})/\phi V_{\text{si}}$ measured on a MCS_I/C sample ($\phi = 0.07$) and a MCS_III/C sample ($\phi = 0.10$). We have added the experimental data measured on a MCS_II/H sample having a silica concentration of 0.10.

At low q value ($qD_{\text{mean}} < 3$), the scattered intensity of the MCS_III/C is larger than the one of the MCS_I/C sample indicating the presence of aggregates in the MCS_III/C samples. Moreover the scattered intensity is slightly larger than the one measured on the MCS_II/H sample having the same silica concentration. The aggregates contained in the MCS_III/C samples seem thus to be larger than the ones existing in the MCS_II/H samples.

More informations about the size of the aggregates can be obtained considering the structure factor of the MCS_III/C samples. In the inset of Fig. 6, one observed a broad shoulder at $q_1 D_{\text{mean}} = 2\pi$ i.e. at a wave vector close to the one corresponding to the particle diameter corresponding to the center-to-center distance of close packed spheres. According to the simulations made by Oberdisse et al. in [19], the shoulder at $q = q_1$ would be the signature of the intra-aggregate contribution $S_{\text{intra}}(q)$ of the structure factor. Moreover we observed a large structure peak at very low q ($q_2 D_{\text{mean}} = 1.5$ for $\phi = 0.1$ and $q_2 D_{\text{mean}} = 1.9$ for $\phi = 0.18$). The peak observed at q_2 is due to the inter-aggregate structure factor. Its position is shifted to lower q values and its amplitude decreases as silica concentration increases. A similar decrease of the intensity at low q with increasing silica concentrations was also observed by Oberdisse et al. [18] on badly dispersed silica/latex systems prepared at $\text{pH} = 5.0$. They concluded that such a decrease of the relative intensities for increasing ϕ is due to a growing up of the aggregate size for increasing silica concentration. Then the aggregate size of the MCS_II/H samples would increase with the silica concentration. If we suppose a liquid-like order between aggregates, the correlation peak of the inter-aggregate structure factor at q_2 is related to the average distance D_2 between aggregates: $q_2 = 2\pi\alpha/D_2$ where α characterizes the degree and the type of positional order of the aggregates. We will assume that the aggregates have a cubic lattice order. In this case, the parameter α is equal to 1 and the peak of the structure factors is related to the aggregation number N_{agg} characterizing the aggregate size: $N_{\text{agg}} = (2\pi/q_2)^3 \phi/V_{\text{si}}$. We can then give from the value of q_2 a rough estimation of the average

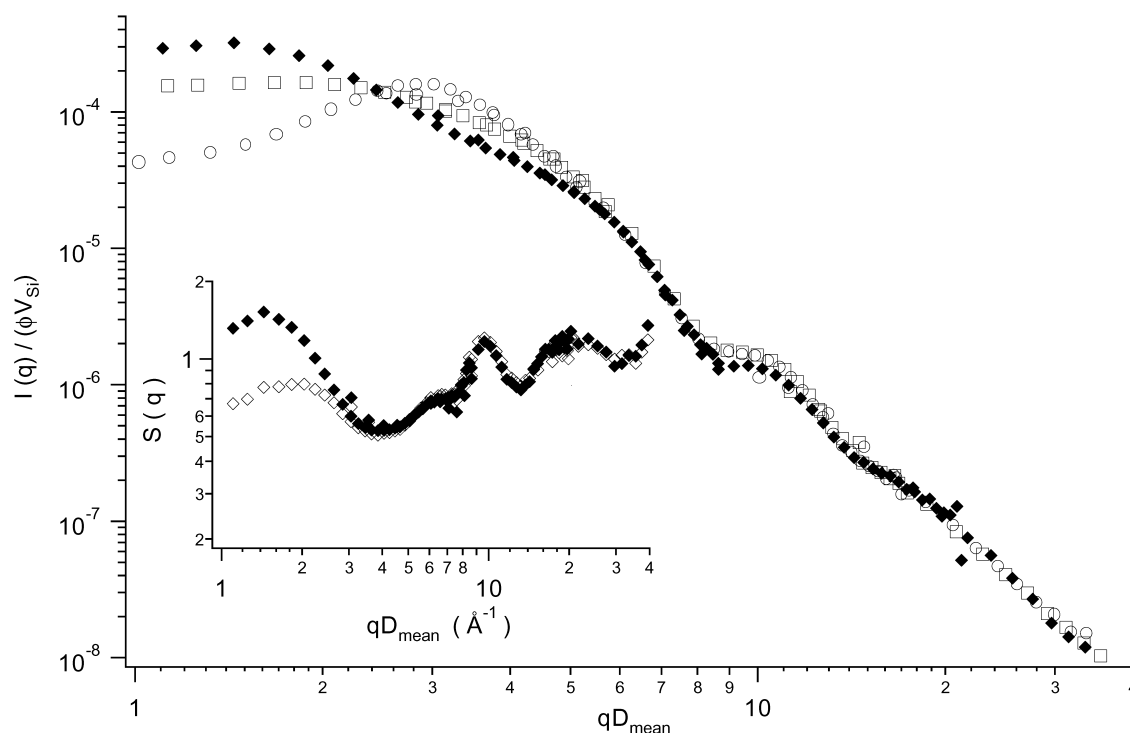


Fig. 6. Comparison of the normalized intensities $I(qD_{\text{mean}})/\phi V_{\text{si}}$ measured on one MCS_III/C sample ($\phi = 0.10$ (\blacklozenge)), one MCS_I/C sample ($\phi = 0.07$ (\circ)) and one MCS_II/H sample ($\phi = 0.10$ (\square)). Inset: structure factors of two MCS_III/C samples: (\diamond): $\phi = 0.18$ and (\blacklozenge) $\phi = 0.10$.

aggregate size for the two MCS_III/C samples. We found $N_{\text{agg}} = 12$ and $N_{\text{agg}} = 18$ for $\phi = 0.10$ and $\phi = 0.18$.

As the particle surface is only partially covered by the grafted molecules, the formation of aggregates is not hindered leading to the presence of aggregates. As the grafting density is high enough, there is no formation of aggregates within the sample.

3.2.2.3. Influence of the grafted molecules reactivity with the acrylate monomers. In this section we analyze how the final dispersion state of our reinforced samples is changed by the reactivity of the grafted molecules with the acrylate monomers during the polymerization step. We compare thus samples obtained after the same concentration step but reinforced with silica particles grafted with molecules able or not to form covalent bonds with the acrylate monomers. We compare samples of the MCS_I/C set with those from the ACS/C family.

Whereas the sample of the all others families were transparent, the reinforced elastomers of the ACS/C set are opaque (of milky aspect). This feature indicates that the particles assemble in large aggregates in these ACS/C samples. The SANS measurements confirm that the dispersion state of the silica is worse than those of the previous filled samples. Fig. 7 shows the relative scattered intensities observed with one ACS/C sample and one MCS_III/H sample containing a silica volume fraction of 0.18. The structure factors $S(q)$ of two ACS/C samples having 0.1 and 0.18 silica in volume are presented in the inset of Fig. 7.

At the low q values ($qD_{\text{mean}} < \pi$), we observed a strong increase of the structure factors after a minimum at $qD_{\text{mean}} \approx 3.5$. The minima are deeper than these, observed previously on the MCS_III/C samples. Moreover the structure factor varies as $q^{-2.5}$. Thus, in this ACS/C family, there are large and compact agglomerates. Their presence is due to the depletion induced by the polymer chains during the polymerization step. Contrary to the other systems, the particles are not connected to the polymer chains. They can move under the depletion effect of the polymer chains during the polymerization step. It is corroborated by the fact that the colloidal solution is transparent before the polymerization and becomes opaque during this step. The opacity does not increase continuously during the polymerization but increases suddenly, before the gel point is reached.

4. Discussion

We evidenced four kinds of samples. The two first classes of samples correspond to systems composed of silica particles totally covered by grafted molecules reacting with the acrylate monomers. First, there are the samples having very good dispersion states with particles surrounded by an exclusion radius. This is the case of the MCS_I/C and TPM_III/C sets. The reinforced elastomers of the second class—samples of the MCS_II/H, TPM_I/H, TPM_II/H—contain some aggregates. The third category corresponds to elastomers reinforced with partially covered particles. The

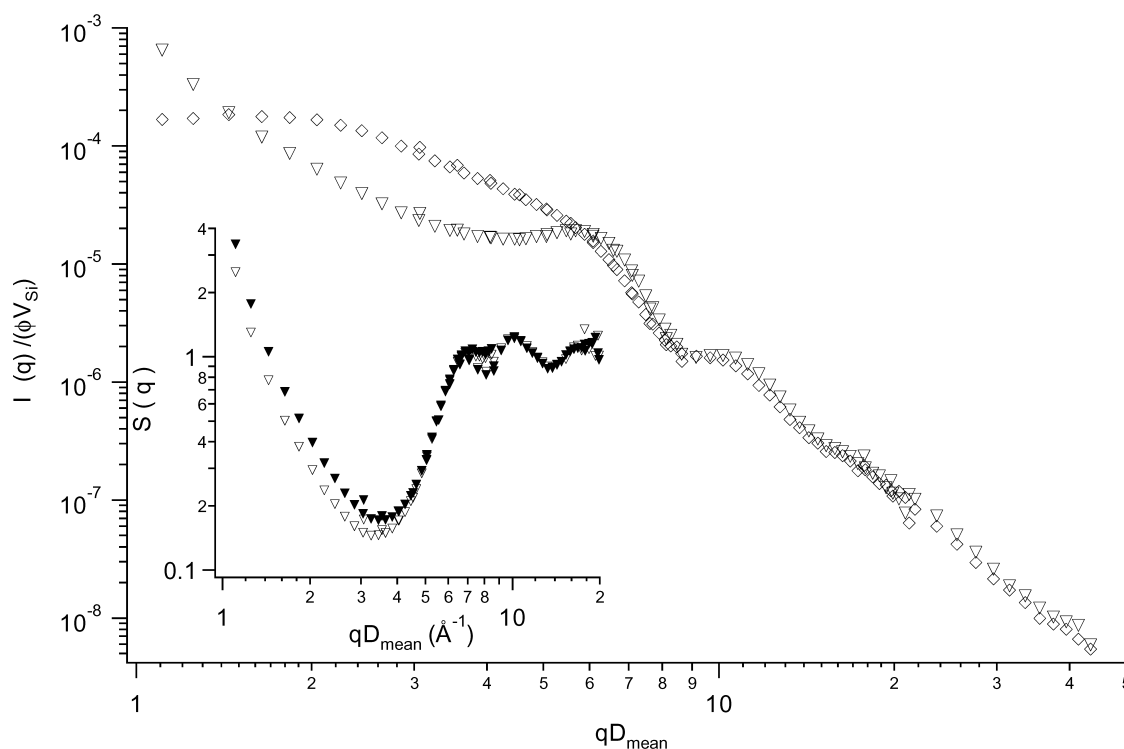


Fig. 7. Comparison of the normalized scattering intensities $I(qD_{mean})/\phi V_{si}$ obtained from one ACS/C sample (Δ) and one MCS_III/C sample (\diamond) having the same silica concentration $\phi = 0.18$. The structure factors of two ACS/C samples are shown in the inset: (\blacktriangledown): $\phi = 0.10$ and (∇): $\phi = 0.18$.

last kind of systems corresponds to samples containing silica particles totally covered by grafted molecules unable to form a covalent bond with the acrylate monomers. These systems have very bad dispersion states and contain large agglomerates (ACS/C samples).

We observed during the polymerization step the competition between two opposite interactions. There are first attractive interactions which are induced by the depletion occurring during the polymerization. Such phenomenon was already predicted by Henderson et al. [20] who showed that a depletion of the polymer density around colloidal particles occurs during a polymerisation. They show that the potential of mean force between colloid particles varies during a polymerization: the contact attraction becomes slightly weaker but the first maximum of repulsion strongly decreases as the degree of polymerisation increases. Furthermore they observe that the attractive region is larger for longer chains. Henderson et al. deduce that polymerization favors particle aggregation. This mechanism is particularly obvious in our systems when there are no covalent bonds between the particles and the polymer chains. This depletion is macroscopically visible: the samples which are transparent before the polymerization become suddenly opaque during the polymerization. The fact that we do not observe a continuous increase of the opacity of the sample during the polymerisation indicates that the depletion occurs as the polymer clusters are large enough compared to the particle diameter. We experimentally observed that this mechanism occurs before the

formation of a gel phase when the viscosity of the colloidal suspension is still low. The depletion stops when the viscosity becomes too large i.e. after the formation of polymer chains network.

These attractive interactions are balanced by repulsive forces of steric nature. During the polymerization, as the coupling agent can form covalent bonds with the acrylate monomers—such as TPM or MCS grafting agents—, polymer chains grow from the particle surface and form a layer surrounding the particle. This polymer shell avoids contacts with other silica particles.

The relative weight of these two opposite interactions depends on the nature of the coupling agent. As this latter can react with the acrylate monomers, the repulsive forces are dominant. Very good dispersion states are observed and the silica particles are surrounded by an exclusion radius sensibly larger than the particle radius. As the graft agent can not form a covalent bond with the acrylate chains (ACS), the attractive depletion forces control the silica arrangement in the elastomer matrix. The amplitude of the depletion decreases as the coupling agent molecules react with the acrylate chains. In this case the motions of the particles should be sensibly slowed down due to their connections with growing polymer clusters.

The aggregates resulting of this depletion mechanism are compact. The formation of compact aggregates induced by a depletion was already observed by Burn et al. [22] or Poon et al. [21] with colloidal suspensions mixed to non-adsorbing polymer chains. They show that, in this case,

dense structures are obtained for slow growth conditions [22]. We deduce that, despite the presence of large polymer clusters in the solution as the depletion occurs, the viscosity of our systems is low enough in order that the particles under the osmotic pressure move and form aggregates. This mechanism agrees with our experimental observations indicating that the viscosity of the colloidal solution is still low as the depletion occurs. The fact that the aggregates are compact shows that the polymer network formation is slow enough compared to the particle rearrangement motions necessary so that dense aggregates are built [22].

Moreover, we observed that samples prepared from a parent concentrated solution obtained after a distillation at 50 °C contains some aggregates. We deduce that the repulsive forces existing between particles in the solution of acrylate monomers are weakened during the distillation performed at 50 °C. We do not observe the formation of compact aggregates. Silica aggregates with low fractal dimension ($d_F \approx 1$) are irreversibly formed during this step. The origin of the aggregate formation during the distillation step is still unknown.

We do not observe differences between the TPM and MCS coupling agents as long as the particle surface is totally covered by coupling agent molecules. As the grafting is partial, larger aggregates are formed before the polymerisation. In this case, there are additional attractive interactions between the particles leading to the formation of aggregates. We did not study in this work the relative weights of the different effects (partial grafting, distillation, depletion) controlling in this case the aggregates formation.

5. Conclusion

We have prepared model filled elastomers using and adapting the method developed by Ford et al. [11]. This method consists in polymerizing a colloidal suspension of grafted silica particles in acrylate monomers. From an initial parent concentrated solution, samples with varying particle volume fractions were prepared. We show in this work that the dispersion state of the filled samples depends on the concentration procedure and on the nature of the coupling agent. We found that the repulsive interactions between the particles remain during a concentration step made by dialysis while they are weakened during a distillation at 50 °C. This latter observation is not yet understood. Moreover, if the particles are not connected to the polymer chains, a depletion mechanism occurs during the polymerization and modifies the dispersion state of the initial solution. The depletion is avoided if the grafted molecules form covalent bonds with the polymer chains. Several filled samples with varying dispersion state and particle/matrix interface were then prepared. By keeping the same particle/

matrix interactions samples it is possible to prepare samples having different dispersion states. We will report in future papers how the swelling and the mechanical properties of these reinforced elastomers are influenced by both parameters. The characterization of the dispersion state by SANS measurements is compulsory to understand the influence of the distribution of the particle–particle distance on the mechanical properties of these model filled elastomers.

Acknowledgements

To D. Dupuis, CRA Rhodia (Aubervilliers-France) who provided us batches of silica particles and to J.L. Halary and A. Dubault for their support in this work. Special thanks to L. Monnerie who is at the origin of this work devoted to the understanding of the mechanical properties of these model reinforced systems.

References

- [1] Wang MZ. *Rubber Chem Technol* 1999;71:520.
- [2] Dannenberg EM. *Rubber Chem Technol* 1986;59:512.
- [3] Wolf S, Wang J, Tan EH. *Kautschuk Gummi Kunststoffe* 1994;47:780. Wolf S, Wang J, Tan EH. *Kautschuk Gummi Kunststoffe* 1994;47:102.
- [4] Aranguren M, Mora E, Macosko C, Saam J. *Rubber Chem Technol* 1995;67:820.
- [5] Funt J. *Rubber Chem Technol* 1988;61:842.
- [6] Medalia AI. *Rubber Chem Technol* 1972;46:653.
- [7] Cembrola RJ. *Polym Engng Sci* 1982;22:601.
- [8] Hess W, Swor RA, Micek EJ. *Rubber Chem Technol* 1984;57:959. Hess W, Swor RA, Micek EJ. *Rubber Chem Technol* 1991;64:386.
- [9] Karasek L, Sumita M. *J Mater Sci* 1996;31:281.
- [10] Zhang Y, Ge S, Tang B, Koga T, Rafailovich MH, Sokolov JC, et al. *Macromolecules* 2001;34:7056.
- [11] Sunkara HB, Jethmalani JM, Ford WT. *Chem Mater* 1994;6:362. Jethmalani JM, Ford WT. *Chem Mater* 1996;8:2138. Jethmalani JM, Ford WT. *Langmuir* 1997;13:3338. Jethmalani JM, Sunkara HB, Ford WT. *Langmuir* 1997;13:2633.
- [12] Pu Z, Mark JE, Jethmalani JM, Ford WT. *Chem Mater* 1997;9:2442.
- [13] Stöber W, Fink A, Bohn E. *J Colloid Interf Sci* 1968;26:62.
- [14] Joseph R, Zhang S, Ford WT. *Macromolecules* 1996;29:1305.
- [15] Berriot J, Lequeux F, Montes H, Pernot H. *Polymer* 2002;43:6131.
- [16] Berriot J, Lequeux F, Monnerie L, Montes H, Long D, Sotta P. *J Non-Cryst Solids* 2002;307–310:719.
- [17] Berriot J, Martin F, Montes H, Sotta P. *Polymer* 2003;44:1437.
- [18] Oberdisse J, Demé B. *Macromolecules* 2002;35:4397.
- [19] Oberdisse J, Rharbi Y, Boue F. *Comp Theor Polym Sci* 2000;10:207.
- [20] Henderson D, Kovalenko A, Pizio O, Wasan D. *Physica A* 1997;245:276.
- [21] Poon WCK, Pirie AD, Pusey PN. *Faraday Discuss Chem Soc* 1995;101:65.
- [22] Burns JL, Yan YD, Jameson GJ, Biggs S. *Colloids Surf: A* 2000;162(1):265. Burns JL, Yan YD, Jameson GJ, Biggs S. *Langmuir* 1997;13(24):6413. Burns JL, Yan YD, Jameson GJ, Biggs S. *Chem Engng J* 2000;80(1–3):23.